THE JOURNAL OF BIOLOGICAL CHEMISTRY VOL. 282, NO. 2, pp. 1051–1058, January 12, 2007

ATP6 Homoplasmic Mutations Inhibit and Destabilize the Human F_1F_0-ATP Synthase without Preventing Enzyme Assembly and Oligomerization*[S]

Received for publication, July 18, 2006, and in revised form, November 1, 2006 Published, JBC Papers in Press, November 22, 2006, DOI 10.1074/jbc.M606828200

Paulina Cortés-Hernández[‡1], Martha E. Vázquez-Memije[§], and José J. García[‡¶2]

From the [‡]Department of Biochemistry, Instituto Nacional de Cardiología "Ignacio Chávez", Mexico City 14080 and the [§]Department of Genetics, Centro Médico Nacional "Siglo XXI," and [¶]Cardiovascular Disease Genomic and Proteomic Study Group, Instituto Nacional de Cardiología "Ignacio Chávez", Mexico City 14080, México

The molecular pathogenic mechanism of the human mitochondrial diseases neurogenic ataxia and retinitis pigmentosa and maternally inherited Leigh syndrome was determined in cultured human cells harboring homoplasmic T8993G/T8993C point mutations in the mitochondrial *ATP6* gene, which encodes subunit 6 of the F_1F_0-ATP synthase. Immunoprecipitation and blue native electrophoresis showed that F_1F_0-ATP synthase assembles correctly in homoplasmic mutant mitochondria. The mutants exhibited a tendency to have an increased sensitivity to subsaturating amounts of oligomycin; this provided further evidence for complete assembly and tight coupling between the F_1 and F_0 sectors. Furthermore, human ATP synthase dimers and higher homo-oligomers were observed for the first time, and it was demonstrated that the mutant enzymes retain enough structural integrity to oligomerize. A reproducible increase in the proportion of oligomeric-to-monomeric enzyme was found for the T8993G mutant suggesting that F_1F_0 oligomerization is regulated *in vivo* and that it can be modified in pathological conditions. Despite correct assembly, the T8993G mutation produced a 60% inhibition in ATP synthesis turnover. *In vitro* denaturing conditions showed F_1F_0 instability conferred by the mutations, although this instability did not produce enzyme disassembly in the conditions used for determination of ATP synthesis. Taken together, the data show that the primary molecular pathogenic mechanism of these deleterious human mitochondrial mutations is functional inhibition in a correctly assembled ATP synthase. Structural instability may play a role in the progression of the disease under potentially denaturing conditions, as discussed.

The F_1F_0-ATP synthase is a ubiquitous enzyme that works as a rotary motor, harnessing the electrochemical proton gradients to carry out ATP synthesis from ADP and P_i. It is composed of a membrane-embedded proton-translocating sector (F_0), coupled to a soluble sector (F_1) that contains catalytic sites for ATP synthesis/hydrolysis. Several of the most deleterious human mitochondrial diseases, such as the maternally inherited Leigh syndrome (MILS)[3] (1, 2), neurogenic ataxia and retinitis pigmentosa (NARP) (3), and some cases of Leber hereditary optic neuropathy (4), are caused by point mutations in the mitochondrial *ATP6* gene that encodes subunit 6 of the ATP synthase F_0 sector.

The same single point mutation can produce either MILS or NARP, depending on the mtDNA mutation load (1, 5, 6). The mtDNA mutations most frequently associated with NARP or MILS are T8993G, T8993C, T9176G, and T9176C, which replace the conserved leucine residues at positions 156 or 217 of subunit 6 by arginine or proline, respectively (6, 7).

NARP/MILS mutations inhibit ATP synthesis (5–77%) and hydrolysis (0–14%) in isolated mitochondria from patient cells (8–12). A similar inhibition is observed when these mutations are modeled in *Escherichia coli* (13–15). The substitution of Leu-156 by arginine (mutation T8993G) is more deleterious to ATP synthesis than its substitution by proline (mutation T8993C) (60 *versus* 25% inhibition in human mitochondria) (6, 8) and therefore leads to more severe NARP/MILS manifestations (16–19). In addition, mitochondria bearing the T8993G mutation are hyperpolarized (9, 20) and have an increased production of reactive oxygen species (20). These functional defects could be caused either by impairment of enzyme assembly or by proton conduction blockade in a completely assembled enzyme. In both scenarios, there would be fewer functional F_0 sectors, and thus ATP synthesis inhibition would occur.

Topology models indicate that NARP/MILS mutations cluster in the most conserved region of human subunit 6 (6, 7, 21), which is involved in proton flux through F_0 (22, 23). The core of this conserved region is an essential arginine residue (Arg-159 in the human enzyme) that undergoes a sequential interaction with the essential carboxyl in each c subunit during enzyme rotation and proton translocation (24). Thus, NARP/MILS mutations could hinder proton translocation by charge redis-

* This work was supported by CONACyT Grants J34744-N and V43814-M, México. The costs of publication of this article were defrayed in part by the payment of page charges. This article must therefore be hereby marked "*advertisement*" in accordance with 18 U.S.C. Section 1734 solely to indicate this fact.

[S] The on-line version of this article (available at http://www.jbc.org) contains supplemental Figs. S1–S3.

[1] CONACyT fellow.

[2] To whom correspondence should be addressed: Dept. de Bioquímica, Instituto Nacional de Cardiología "Ignacio Chávez," Juan Badiano 1 Sección XVI, México DF 14080. Tel.: 55-73-29-11 (Ext. 1517); Fax: 55-73-09-26; E-mail: jjgarcia_trejo@yahoo.com.

[3] The abbreviations used are: MILS, maternally inherited Leigh syndrome; BN-PAGE, blue native-PAGE; IF_1, F_1-ATPase inhibitor protein; NARP, neurogenic ataxia and retinitis pigmentosa; OSCP, oligomycin sensitivity conferring protein; RFLP, restriction fragment length polymorphism; SMP, submitochondrial particles; BisTris, 2-[bis(2-hydroxyethyl) amino]-2-(hydroxymethyl)propane-1,3-diol.

tributions or subtle structural changes in the interface of subunit 6 and the barrel of c subunits (7, 9).

On the other hand, the transmembrane location of NARP/MILS mutations may induce subunit mis-folding and interfere with the assembly of the complete F_1F_0. In this scenario soluble F_1 and incomplete F_1F_0 complexes would be found in mitochondria, as reported for mtDNA-less Rho^0 cells lacking *ATP6* and *ATP8* (9, 25). Incomplete F_1F_0 complexes have been found in postmortem heart tissue from MILS patients (26), in NARP/MILS cybrids (27), and in skeletal muscle biopsies from these patients (25). In contrast, a normal content of F_1F_0 subunits, including subunit 6, was found in the enzyme isolated from patient cultured fibroblasts (9). To establish the molecular mechanism through which NARP/MILS mutations induce disease, it is crucial to determine unambiguously whether these point mutations impair F_1F_0 assembly.

Most of the previous structural studies have been done with heteroplasmic cells, where wild type and mutant *ATP6* genes are co-expressed. To avoid wild type complementation in ATP synthase assembly or function, we used homoplasmic T8993G and T8993C cultured human cells to assess conclusively the effect of these mutations on the assembly of the ATP synthase. A novel immunoprecipitation procedure (28) was instrumental to isolate the whole F_1F_0 complex from human mitochondria. In parallel, blue native electrophoresis (BN-PAGE) (29) was used to estimate the amounts of native F_1F_0 complexes in wild type and mutant mitochondria.

The eukaryotic F_1F_0-ATP synthase forms homodimers (30–32) and larger oligomers (33) that contribute to mitochondrial cristae morphology (34). To date, this oligomerization has not been studied for the human enzyme. Here we demonstrate that *ATP6* mutations do not impair dimerization and homo-oligomerization of the human F_1F_0. Functional and instability defects produced in the whole F_1F_0 by these mutations are assessed and discussed.

EXPERIMENTAL PROCEDURES

Cell Cultures—T8993G and T8993C patient skin fibroblasts were kindly provided by Professor Brian H. Robinson (Hospital for Sick Children, Toronto, Canada). Control human MRC5 fibroblasts were purchased from In Vitro S.A. Homoplasmic T8993G cybrids (produced by the fusion of enucleated patient skin fibroblasts with Rho^0 143B/TK^- osteosarcoma cells) and control Rho^+ 143B/TK^- osteosarcoma cells were derived from cell cultures at the laboratory of Prof. Rosalba Carrozzo, as described in Ref. 20. Cell culture was carried out in high glucose media, as described before (9), but in the presence of antibiotics (100 units/ml penicillin G, 100 μg/ml streptomycin sulfate, and 2 μg/ml amphotericin B) from Invitrogen.

Antibodies—Monoclonal antibodies, 12F4AD8, anti-α, anti-OSCP, and anti-IF_1, were from Mitosciences and were used according to the manufacturer.

DNA Isolation, PCR, and RFLP—Total DNA was isolated from 1×10^6 cells. A segment of the *ATP6* gene was amplified by PCR; products were digested with the endonuclease MspI (Promega) and separated in PAGE for RFLP analysis.

Isolation of Human Mitochondria—Mitochondria were isolated from 180 to 200 $\times$ 10^6 cells by differential centrifugation, as described in Ref. 9. Submitochondrial particles (EDTA-SMP) were prepared by sonication of isolated mitochondria as in Ref. 8.

F_1F_0 immunoprecipitation was carried out from 3 mg of human mitochondria solubilized with *n*-dodecyl-β-D-maltoside (Sigma), as described previously (28). Where indicated, prior to solubilization, human mitochondrial membranes were obtained by subjecting mitochondria to an osmotic shock, as described previously (9).

BN Electrophoresis, Second Dimension SDS-PAGE, and Western Blot—BN-PAGE was as described previously (29). The solubilization buffer consisted of 0.75 M ϵ-aminocaproic acid, 50 mM BisTris-HCl, pH 7. Digitonin or *n*-dodecyl-β-D-maltoside (Sigma) was used for mitochondrial protein extraction. Titration curves were carried out to establish the appropriate detergent amounts to extract intact F_1F_0 complexes in its monomeric and oligomeric forms. ATPase activity was developed in native gels as described previously (34). Single native lanes were submitted to second dimension SDS-PAGE, transferred to polyvinylidene fluoride membranes, and probed with antibodies as described previously (35).

ATP Synthesis and Hydrolysis Assays—Spectrophotometric measurements of ATP synthesis rates coupled to $NADP^+$ reduction were carried out at 340 nm with 30 μg of isolated mitochondria as described (36), including 100 μM diadenosine pentaphosphate to inhibit adenylate kinase activity. Alternatively (see Fig. 5*A*), the phosphorylation of ADP by inorganic phosphate ($^{32}P_i$) was used to determine ATP synthesis (8).

ATP hydrolysis rates were measured spectrophotometrically with mitochondrial membranes obtained by osmotic shock, using an ATP-regenerating system, as described before (9). Where indicated, prior to measurements, mitochondrial membranes were resuspended in "activation conditions" consisting of 125 mM KCl, 2 mM EDTA, 30 mM Tris-SO_4, pH 8.0, and protease inhibitors (0.5 μg/ml leupeptin, 0.5 μg/ml pepstatin, 1 mM phenylmethylsulfonyl fluoride) and incubated at the indicated times at 40 °C to release the inhibitory protein (IF_1). Control "nonactivation conditions" were 0.25 M sucrose, 2 mM EDTA, 10 mM Tris-HCl, pH 7.4 and protease inhibitors (as above). To verify IF_1 release, membranes were pelleted by centrifugation at 15,000 $\times$ *g*, and supernatants were assayed by Western blot for the presence of IF_1. ATP hydrolysis carried out by SMP was measured by the colorimetric determination of P_i released from ATP, as reported (8).

Other Methods—Protein was measured by a modified Lowry method (see Ref. 37). SDS-PAGE was according to Laemmli (38). Densitometry analyses were carried out with Alpha-DigiDoc computer software coupled to a Kodak DC290 digital camera.

RESULTS

T8993G Mutation Loads—We studied two human cell cultures harboring the T8993G mutation, namely skin fibroblasts and cybrids, with their respective controls. The T8993G mutant mtDNA load was determined in each cell culture by RFLP with the endonuclease MspI on a 764-bp *ATP6* gene fragment. The wild type restriction pattern was absent from mutant samples (<1% of total DNA, by densi-

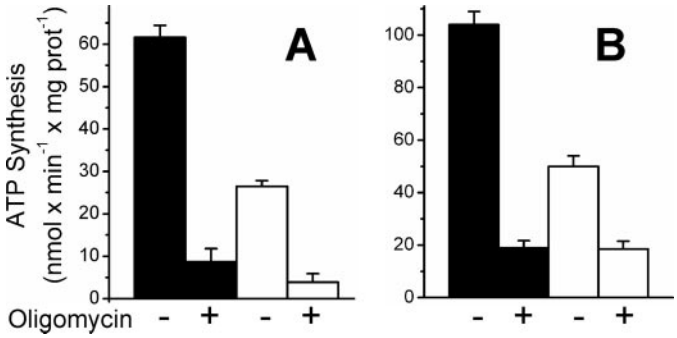

FIGURE 1. **ATP synthase activity of fibroblast (*A*) and cybrid (*B*) isolated mitochondria.** *Black bars* correspond to wild type and *white bars* to homoplasmic T8993G mitochondria. The average and standard deviations of three spectrophotometric determinations with and without oligomycin (10 μg/mg protein) are shown.

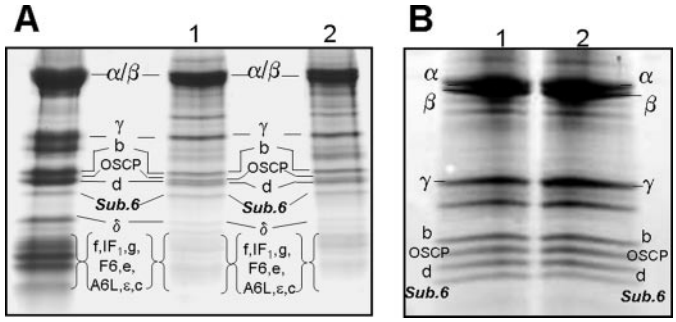

FIGURE 2. **SDS-PAGE of F_1F_o purified by immunoprecipitation from human (*A*) fibroblasts and (*B*) cybrids.** Wild type and L156R F_1F_o was loaded onto *lanes 1* and *2*, respectively, in a 10–22% SDS gel. Gels were stained with Coomassie. *A*, whole mitochondria were used for immunoprecipitation, and F_1F_o immunoprecipitated from bovine heart mitochondria was included at the *extreme left* for comparison. Subunit γ/6 density ratios were 3.66 for control and 3.70 for mutant. *B*, osmotic shocked mitochondrial membranes were used for immunoprecipitation. The gel was over-run to resolve clearly subunits b, OSCP, d, and 6, although smaller subunits ran off. Subunit γ/6 density ratios were 4.12 and 5.03; whereas b/6 were 2.04 and 2.00 for control and mutant cybrids, respectively. *Sub.6*, subunit 6.

tometry analysis), regardless of the amount of genomic DNA used for amplification (supplemental Fig. 1). Therefore, we confirmed that the cells used in this study are homoplasmic for the T8993G mutation.

Homoplasmic T8993G Mutants Show Decreased ATP Synthesis—Oligomycin-sensitive ATP synthesis rates of homoplasmic T8993G mitochondria decreased to 40% of their respective controls (Fig. 1, *A* and *B*). This further confirms the homoplasmicity of the studied samples, because only the homoplasmic T8993G mutation results in 60% inhibition of ATP synthesis rates (9). Small amounts of wild type mtDNA complement substantially the ATP synthase activity; accordingly, mitochondria with 91% mutant load have only a 25% ATP synthesis inhibition (9). Osteosarcoma mitochondria had 30% higher synthesis rates than those obtained from fibroblasts, probably because of a better yield of coupled mitochondrial membranes. However, the ATP synthesis rates of the four cell types showed a similar inhibition when incubated with saturating concentrations of oligomycin (Fig. 1, *A* and *B*).

Immunoprecipitation of the Human F_1F_o Complex from Homoplasmic Control and T8993G (L156R) Mitochondria—Aggeler *et al.* (28) described a one-step isolation approach to immuno-capture the whole, functional, oligomycin-sensitive F_1F_o complex from small amounts of solubilized human mitochondria with a monoclonal antibody (12F4AD8). Because the antibody recognizes the native F_1 portion,[4] enzyme assembly can be tested with this procedure, *i.e.* in the properly assembled F_1F_o complex, F_o subunits will co-immunoprecipitate with the F_1 portion. By SDS-PAGE of immunoprecipitated samples and band densitometry analyses, it was possible to estimate the ratio of F_o to F_1 subunits. Subunit 6 was present at similar intensity ratios in the immunoprecipitated F_1F_o complexes from control and mutant mitochondria (Fig. 2, *A* and *B*). Thus, assembly of the human F_1F_o-ATP synthase was not prevented by the L156R mutation, neither in fibroblasts (Fig. 2*A*) nor in cybrids (Fig. 2*B*). In both cell types, the protein yields of immunoprecipitated F_1F_o were similar between control and mutant mitochondria.

These results are consistent with those previously obtained with the human ATP synthase isolated by affinity chromatography from heteroplasmic (91%) T8993G mitochondria (9). As in that study, the F_1F_o subunits resolved here were α, β, γ, b, OSCP, d, and subunit 6; however, small subunits of F_1 (ϵ, IF_1) and F_o (e, f, g, F6, A6L, and c) were not resolved.

For the gel shown in Fig. 2*B*, mitochondrial membranes were obtained by osmotic shock prior to solubilization and immunoprecipitation. This improved the purity of the enzyme, and it was useful to analyze the amount of F_1 subunits released from mitochondria by osmotic shock as markers of ATP synthase disassembly. The content of subunits α, OSCP, and IF_1 was similar in the supernatants of shocked control and mutant mitochondria, as shown by Western blot (supplemental Fig. 2). Furthermore, no differences in subunit content or intensity ratios were found between F_1F_o immunoprecipitated from whole or osmotic-shocked mitochondria (not shown). Taken together, these results confirm that the mutant subunit 6 incorporates properly into the fully assembled human F_1F_o-ATP synthase.

Native Electrophoresis of Control, T8993G, and T8993C Mitochondria—We used blue native-PAGE to compare the amounts of native monomeric and oligomeric F_1F_o extracted from control and mutant mitochondria, as an alternative method to check for assembly defects caused by subunit 6 mutations. To compare the effects of leucine 156 substitutions by arginine or proline, we included T8993G (L156R) and T8993C (L156P) human fibroblast mitochondria.

Fig. 3, *A* and *B*, shows the bands corresponding to the native oxidative-phosphorylation complexes I, III, IV and V, obtained from dodecyl maltoside mitochondrial extracts. The band containing F_1F_o (complex V) was assigned by in-gel development of ATPase activity and by the subunit pattern found in second dimension SDS-PAGE (not shown). The complete monomeric F_1F_o was present in similar amounts in control and mutant mitochondria (both L156R and L156P) as confirmed by densitometry ratios of complex V (ATP synthase) and complex III (dimeric bc_1) (Fig. 3, *A* and *B*).

[4] J. J. García, unpublished observations.

To detect small amounts of incomplete F_1F_0 or soluble F_1 as markers of enzyme disassembly, individual BN-PAGE lanes were submitted to second dimension SDS-PAGE and anti-α Western blotting. In control (Fig. 3*C*) as well as in L156R (Fig. 3*D*) mitochondria, α subunits were detected only in two positions of the blot, corresponding to the BN-PAGE migration of monomeric F_1F_0 and F_1, respectively. Equivalent results were obtained for L156P mutants (not shown). These experiments demonstrated that small quantities of F_1 are detectable in human mitochondrial extracts, but these are not increased in mutant samples as compared with controls. Taken together the data confirm that L156R and L156P NARP/MILS mutations do not impair monomeric F_1F_0 assembly.

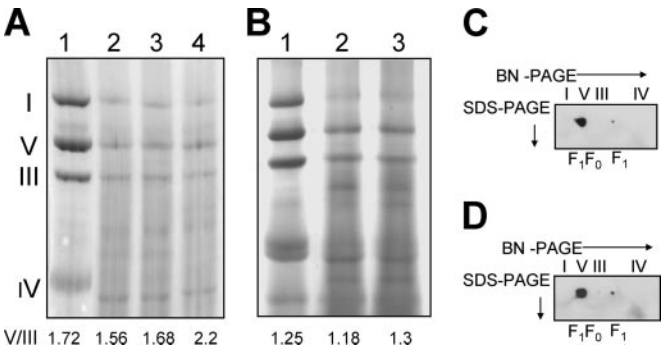

FIGURE 3. **Blue native gel electrophoresis of fibroblast (*A*) and cybrid (*B*) human mitochondria, solubilized with dodecyl maltoside (3 g/g of protein).** For comparison, solubilized bovine heart mitochondria were loaded in *lanes 1*. *Lanes 2* correspond to human control, *lanes 3* to T8993G, and *lane 4* to T8993C mitochondria. The ratio of complex V/complex III densities is indicated at the *bottom* of each lane. *C* and *D* show α subunit immunoblots of second dimension SDS-PAGE from control osteosarcoma and T8993G cybrids, respectively. The migration of each oxidative-phosphorylation complex in the native-PAGE, is depicted at the *top* of the blots in *roman numerals*.

Mitochondrial F_1F_0 can further assemble into dimers (30, 32) and higher oligomers (33) that control cristae morphology. Therefore, to explore F_1F_0 oligomerization in the L156R/L156P human mutants, mitochondrial digitonin extracts were subjected to BN-PAGE, followed by second dimension SDS-PAGE and α subunit immunodetection. The α subunits were found at the positions corresponding to the migration of F_1F_0 supercomplexes (V_n) (31) and monomeric F_1F_0 (V) in BN-PAGE (Fig. 4, *A–E*). The identity of the supercomplexes as ATP synthase homo-oligomers was corroborated by parallel analyses of bovine heart mitochondria (not shown). From the several oligomeric forms of the human ATP synthase detected, the most abundant had an apparent mass of 1400 kDa and migrated between the monomeric complex I (1000 kDa) and the supercomplex composed by I + III_2 (1500 kDa), thus corresponding to dimeric F_1F_0. This dimer dissociated progressively as the digitonin concentration was raised in parallel to an enrichment of monomeric F_1F_0 (Fig. 4, *A–E*). On the other hand, larger F_1F_0 oligomers showed a lower mobility than the I + III_2 supercomplex (see *far left side* of Fig. 4, *A–C*) and therefore are likely composed by ATP synthase trimers and/or tetramers. However, formation of ATP synthase hetero-oligomers, *i.e.* associations with other mitochondrial proteins such as adenine nucleotide and P_i carriers as in the ATP synthasome (39), is also possible. These larger ATP synthase oligomers had a better resistance to dissociate with increasing digitonin concentrations than the dimer. In osteosarcoma mitochondrial extracts, these oligomers seem absent (Fig. 4, *D* and *E*); however, further BN-PAGE and two-dimensional PAGE analyses are required to determine whether these apparent differences simply reflect a lower electrophoretic resolution of the osteosarcoma mitochondrial extracts. Alternatively, these differences could reflect changes in protein expression and/or lipid content between control and osteosarcoma mitochondrial preparations. To avoid errors in the densitometric estimations derived from variations in electrophoretic resolution, the densities of all ATP synthase oligomers observed were added together in a single composed density. This is indicated in Fig. 4, *A–E* as "V_n."

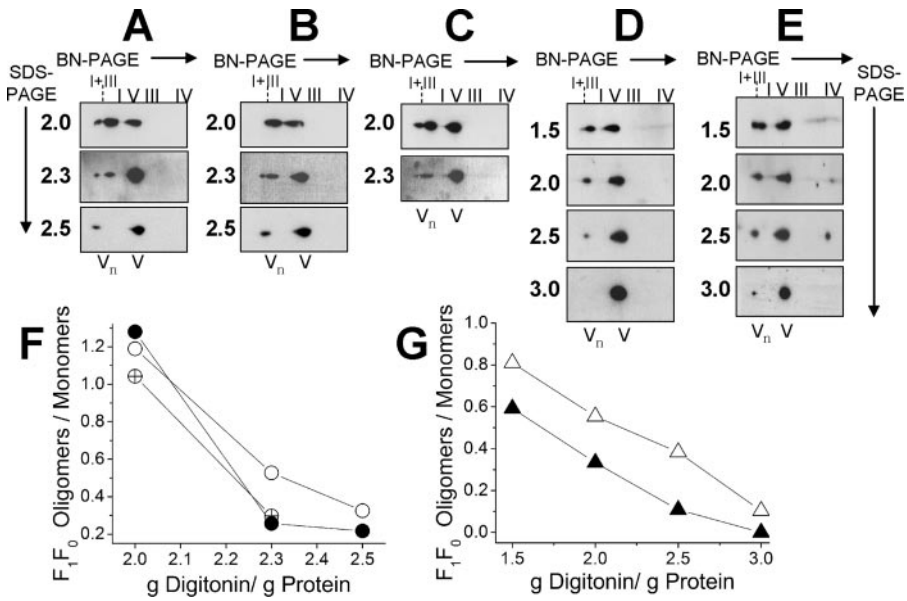

FIGURE 4. **Immunodetection of human F_1F_0 oligomers.** *A–E* are anti-α Western blots of digitonin mitochondrial extracts separated by BN-PAGE and second dimension SDS-PAGE. The migration of each oxidative-phosphorylation complex in BN-PAGE is depicted at the *top* of the blots in *roman numerals*. *I + III* indicates the migration of the supercomplex containing complex I and dimeric complex III. *A–C* correspond to control, T8993G, and T8993C fibroblasts, respectively, whereas *D* and *E* are control osteosarcoma and T8993G cybrids. *Arabic numbers* at the *left* of each blot indicate digitonin/protein ratios (w/w). Oligomeric (V_n) and monomeric (V) enzyme proportions were obtained by densitometry and plotted against detergent amount per protein for fibroblasts and cybrids in *F* and *G*, respectively. *Filled symbols* represent control and *open symbols* represent T8993G mutants. *Crossed circles* in *F* belong to T8993C mutant fibroblasts.

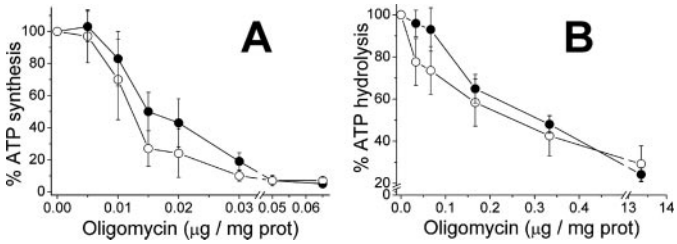

FIGURE 5. **Oligomycin sensitivity of ATP synthesis (*A*) and ATP hydrolysis (*B*) of control osteosarcoma (*filled circles*) and T8993G cybrids (*open circles*).** The indicated oligomycin amounts per protein were added to mitochondrial membranes and incubated for 5 min at 37 °C, prior to activity determinations. Percent inhibition is shown. The 100% values (nmol × min^{-1} × mg $protein^{-1}$) were 103 ± 35 and 24 ± 17 (ATP synthesis) and 412 ± 37 and 326 ± 42 (ATP hydrolysis), for control and mutant respectively. The average and standard deviations of four and three determinations are shown in *A* and *B*, respectively.

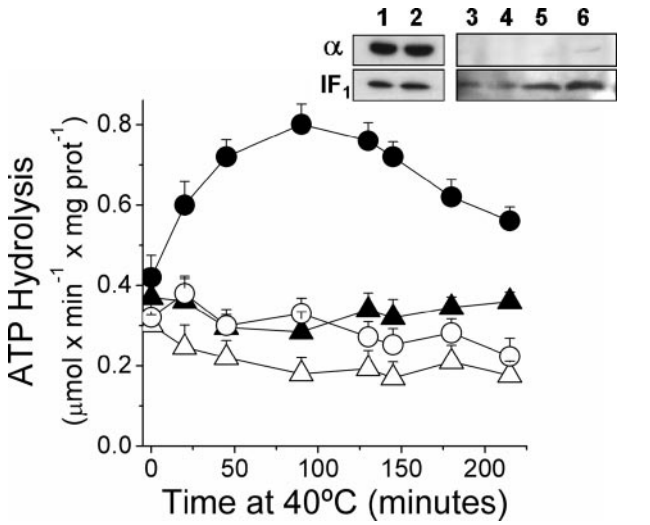

FIGURE 6. **Time course activation of ATP hydrolysis in mitochondrial membranes from control osteosarcoma (*filled symbols*) and T8993G mutant cybrids (*empty symbols*).** Mitochondrial membranes were incubated at 40 °C either in activation conditions (*circles*) or in nonactivation conditions (*triangles*); at each time, an aliquot was used to measure ATP hydrolysis. Oligomycin-insensitive ATP hydrolysis was subtracted from each point. The average and standard deviation of three experiments is shown. *Inset*, α and IF_1 subunits were detected by Western blot. Control and L156R whole mitochondria are shown in *lanes 1* and *2*, respectively. Supernatants of control and L156R membranes incubated for 90 min in nonactivation conditions are shown in *lanes 3* and *4*, and those incubated in activation conditions are shown in *lanes 5* and *6*. α subunits were nearly undetectable in these supernatants. IF_1 to α densitometry ratios for the *1st two lanes* were 0.47 and 0.57, respectively.

chondria. This procedure was instrumental for comparing by densitometry the proportion of oligomeric (V_n) and monomeric (V) F_1F_0 between *ATP6* mutants and their controls. The oligomer-to-monomer ratios (V_n/V) are plotted in Fig. 4, *F* and *G*, for fibroblasts and cybrids, respectively. The results show that the L156R/L156P mutations do not impair dimerization or higher order oligomerization of the human F_1F_0-ATP synthase. Rather, a tendency to increase F_1F_0 oligomerization was observed in mitochondria harboring the L156R homoplasmic mutation (Fig. 4, *F* and *G*). Mitochondria solubilized from different preparations at 1.5 g of digitonin/g of protein had an average oligomer-to-monomer ratio of 0.62 ± 0.11 for control and 1.47 ± 0.43 for L156R cybrids ($n = 5$, representative experiments are shown in Fig. 4 and supplemental Fig. 3).

Oligomycin Sensitivity in T8993G and T8993C Mutants—Based on studies on heteroplasmic T8993G cells, some groups (11, 40) propose that the pathogenic mechanism of NARP/MILS is a partial uncoupling of F_0-proton translocation from F_1-ATP synthesis. We evaluated functional coupling between F_1 and F_0 sectors in the homoplasmic T8993G cybrids by assaying oligomycin sensitivity during ATP synthesis and hydrolysis (Fig. 5, *A* and *B*). Oligomycin binds to F_0, blocking the proton channel and thus inhibiting F_1 catalysis in a well coupled enzyme. As shown in Fig. 5, *A* and *B*, the L156R mutant and control enzymes showed similar oligomycin sensitivities in both activities measured. However, the L156R mutant had a trend to show a higher oligomycin sensitivity that is more evident at oligomycin amounts around 0.02 μg/mg protein. This tendency is in consonance with the higher oligomycin sensitivity reported previously for ATP synthesis in fibroblasts with the same mutations (8). A similar trend was also observed with mitochondria isolated from human fibroblasts harboring the L156R/L156P mutations (not shown). These experiments provide further evidence of the tight coupling that exists between F_1 and F_0 sectors in the mutant enzyme preparations studied here.

F_1F_0 Destabilization in T8993G (L156R) Mutants—Because no F_1F_0 assembly defects were found in mitochondria from NARP/MILS mutants, we compared the functional and structural stability of the wild type and L156R mutant F_1F_0 by incubation in potentially destabilizing conditions. When F_1F_0-ATPase activity was measured in conditions of maximal turnover ("activation conditions," *i.e. in vitro* conditions that release the inhibitory subunit IF_1), the L156R mutants failed to increase their hydrolytic activities as the wild type does (Fig. 6). The time course of activation showed a classical bell-shaped curve for the wild type enzyme, corresponding to the balance between enzyme activation by IF_1 release and enzyme inactivation that becomes evident after 90 min. In contrast the mutant did not show activation but only a tendency to inactivate along the whole time course. As shown in Fig. 6 (*inset*), the mutant and wild type whole mitochondria had a similar IF_1 content (see α/IF_1 ratios for *lanes 1* and *2*), and both mitochondrial membranes released a similar amount of IF_1 to the supernatant after a 90-min incubation at 40 °C in activation conditions (*lanes 5* and *6*). Thus, the lack of activation in the mutant F_1F_0 is not a result of IF_1 overexpression or failure to release IF_1. We therefore looked for structural F_1F_0 alterations associated with the lack of mutant activation. Control and L156R mutant mitochondrial membranes were activated during 90 min; afterward dodecyl maltoside extracts of "activated" and "nonactivated" membranes were obtained. These extracts were subjected to BN-PAGE, second dimension SDS-PAGE and immunodetected for α and IF_1 subunits. Nonactivated wild type and mutant membranes showed a similar content of native monomeric F_1F_0, as revealed by the migration of α subunits (Fig. 7, *A* and *B*, *upper panels*). IF_1 was detected aligned vertically with α subunits (Fig. 7, *A* and *B*, *lower panels*), indicating that the inhibitory subunit was associated with the control and mutant enzymes in these conditions. A small quantity of F_1 was found in mutant blots (Fig. 7*B*). As expected, after activation, no IF_1 was detectable in association with F_1F_0 (Fig. 7, *C* and *D*, *lower panels*; see figure legend for a detailed description). The acti-

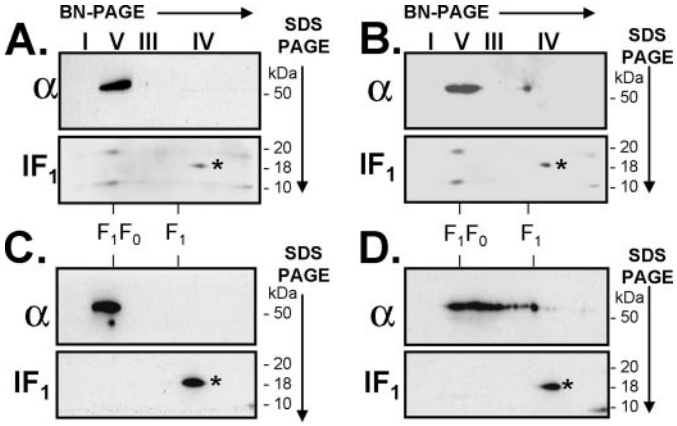

FIGURE 7. **Instability of the L156R monomeric ATP synthase under conditions that release IF_1.** *A* and *C* show control osteosarcoma, and *B* and *D* are L156R cybrids. Nonactivated (*A* and *B*) or activated (*C* and *D*) mitochondrial membranes were separated by BN-PAGE and second dimension SDS-PAGE; α and IF_1 subunits were detected by Western blot. The migration of each oxidative-phosphorylation complex in the native-PAGE is depicted at the *top* of the blots in *roman numerals*. IF_1 forms SDS-resistant homodimers, and it is detected as two bands of 10 and 20 kDa, respectively. In addition, according to the manufacturer, the monoclonal anti-IF_1 antibody cross-reacts with the cytochrome oxidase 18-kDa subunit (marked with an *asterisk*), which in this experiment may be used as reference for the migration of native complex IV. In *C* and *D* no IF_1 was detected, only the overexposed spot corresponding to cytochrome oxidase 18-kDa subunit is seen.

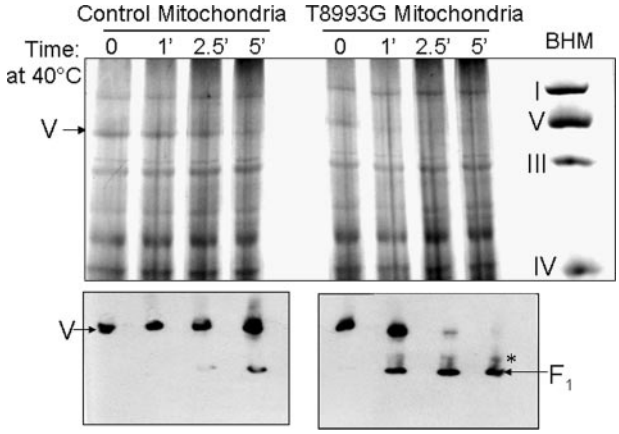

FIGURE 8. **Destabilization of monomeric human F_1F_0 by heat.** *Upper panel,* Coomassie-stained BN-PAGE of dodecyl maltoside (3 g/g of protein) mitochondrial extracts. Human extracts were heated at 40 °C for the indicated minutes prior to gel loading. For comparison, bovine heart mitochondria (*BHM*) were included at the *extreme right*. The migration pattern of the respiratory complexes is indicated with *roman numerals*. *Lower panel* shows α subunit immunodetection in an equivalent BN-PAGE. *V* indicates the monomeric F_1F_0, and the *asterisk* shows an F_1F_0 disassembly intermediate.

vated wild type F_1F_0 was resolved at the same position as without activation (Fig. 7*C*, *upper panel*), showing that it retained its native structure. In contrast, for the L156R mutant incubated in activation conditions, α subunits were found as a smear corresponding to disassembly intermediates containing F_1, along with a small increment in the spot corresponding to soluble F_1 (Fig. 7*D*). Thus the monomeric form of the L156R mutant F_1F_0 is unstable under activation conditions, as compared with the wild type enzyme.

To look for evidence of F_1 release from F_0 under other destabilizing conditions, activated submitochondrial particles (EDTA-SMP) were prepared by sonication from control osteosarcoma and L156R cybrid mitochondria. The ATPase activities that remained in the particles were compared with the activity released to the supernatant. From the total ATPase activity obtained after sonication, 21 and 27% were found in the supernatant of control and L156R SMP after ultracentrifugation, respectively (not shown). In both cases the hydrolytic activity of the supernatants was 75–78% sensitive to the F_1 inhibitor efrapeptin (75 μg/mg protein). Thus, release of F_1 during SMP preparation is slightly higher in mutant mitochondria than in wild type.

As shown in Fig. 5*B*, the ATPase activities from mutant and control mitochondria reached a similar maximal inhibition (around 80%) with saturating oligomycin. In contrast, for EDTA-SMP with saturating amounts of oligomycin (40 μg/mg protein), ATPase activity was inhibited 72% in control, but only 58% in the L156R mutant (not shown), suggesting some enzyme uncoupling because of sonication that is more evident in the mutant.

We next compared the stability of control and L156R mutant monomeric F_1F_0 by incubation of dodecyl maltoside mitochondrial extracts at 40 °C. In these experiments samples were heated directly in the solubilization buffer in which they were extracted and subsequently loaded onto blue native gels. A representative Coomassie-stained native gel is shown in Fig. 8, *upper panel*, and the *lower panel* shows the immunodetection of α subunits in an equivalent native gel. The L156R monomeric ATP synthase (complex V) was readily lost after 2.5 min at 40 °C, yielding F_1 and other disassembly intermediates. In contrast, most of the wild type enzyme resisted a 5-min incubation at 40 °C. It should be noted that the observed disassembly occurred only for complex V in these conditions; complexes I and III remained assembled at the incubation times shown. The F_1F_0 disassembly intermediate marked with an *asterisk* (Fig. 8, *lower panel*) is compatible with those described previously for T8993G mitochondria (25–27), which mainly contain F_1 and c subunits. The detergent present in the samples (3 g of dodecyl maltoside/g of protein) probably accounts for the short times that are sufficient to observe enzyme disassembly in this experiment.

We also analyzed if the dimeric human F_1F_0 is destabilized by *ATP6* mutations. Digitonin extracts that contained dimeric and monomeric F_1F_0 were obtained; aliquots were incubated at 40 °C for 90 min in the solubilization buffer used for extraction and compared in BN-PAGE and SDS-PAGE with their non-heated counterparts. After heating, the ratio of oligomeric-to-monomeric F_1F_0 decreased from 0.64 to 0.33 for the control enzyme and from 1.89 to 0.34 for the L156R mutant (supplemental Fig. 3). This figure also shows that there is a higher IF_1 content in the multimeric F_1F_0 complexes of control and mutant enzymes as compared with the IF_1 amounts associated with monomeric F_1F_0 (supplemental Fig. 3, *A* and *B*). This result is in concordance with the role of IF_1 in promoting dimerization of the whole F_1F_0 complex as found by IF_1 reconstitution or its overexpression in bovine and rat mitochondria or submitochondrial particles (41). Supplemental Fig. 3 also shows that IF_1 is released by heat from monomeric and oligomeric F_1F_0 in both control and mutant enzymes (compare *A* and *B* with *C* and *D*). Furthermore, no smearing of the α-signal was observed after heating, two-dimensional PAGE, and West-

ern blot, probably because the human F_1F_0 monomer and its oligomers are more stable in digitonin (1.5 g/g of protein) than the F_1F_0 monomer in dodecyl maltoside (3 g/g of protein, used in Figs. 7 and 8). Nevertheless, the key result of these experiments is that the monomeric and oligomeric human F_1F_0 complexes are destabilized by *in vitro* denaturing conditions such as mild heating for the detergent-extracted enzyme and sonication or increased salt, temperature, and pH as in the case of the membrane-embedded F_1F_0.

Taken together, the overall results demonstrate that the L156R mutant enzyme is well coupled and assembled in the mitochondria of NARP/MILS patients. However, it is less stable than the wild type under *in vitro* destabilizing conditions.

DISCUSSION

This work solves the controversy of structural *versus* functional pathogenic mechanisms of the *ATP6* mutations that produce NARP/MILS mitochondriopathies in human patients by demonstrating functional inhibition in a well coupled and properly assembled human F_1F_0-ATP synthase carrying subunit 6 mutations.

Among the possible consequences of *ATP6* point mutations, impaired F_1F_0 assembly (26, 27), enzyme uncoupling (11, 40), and proton conduction blockade through F_0 (6, 7, 9) have all been proposed. To distinguish between them, concluding evidence on the effect of NARP/MILS mutations on F_1F_0 assembly was limited because the reported human F_1F_0 structural studies have been done mostly with heteroplasmic cells and provided apparently opposing results (9, 25–27). Here we demonstrate the proper assembly of the F_1F_0 complex in two T8993G homoplasmic human cell cultures, namely fibroblasts and cybrids, by immunoprecipitation (Fig. 2) and direct electrophoretic resolution of the native enzyme (Figs. 3 and 4). Furthermore, tight coupling between the F_1 and F_0 sectors in the L156R mutant enzyme was evidenced by the oligomycin sensitivity found in ATP synthesis and hydrolysis (Fig. 5). Because structural integrity is essential for oligomycin inhibition, this confirmed that the mutant F_1F_0 complex is correctly assembled, even in the presence of >99% T8993G mutated DNA copies.

Cybrids and osteosarcoma control cells share the same nuclear background, which allows focusing on the pathogenic effects of the mtDNA mutation. Nevertheless, we had equivalent results with fibroblasts obtained from patients, which have not been genetically manipulated. The homoplasmicity of the mutant cultures used in this work guaranteed the study of enzymes containing either the normal or the mutated subunit 6, but not a mixture of them.

Additionally, because the ATP synthase dimerizes in mitochondria, mainly through F_0 interactions (30, 32), we studied for the first time the existence of F_1F_0 dimers and higher oligomers in human mitochondria (Fig. 4). Human F_1F_0 oligomerization was not prevented by the mutations studied here. This further confirms the lack of assembly defects in both of the most common NARP/MILS mutations (L156R and L156P) and corroborates that the small F_0 subunits (which were not resolved here by SDS-PAGE) are present in the mutant F_1F_0 complex. These likely include subunits e and g, which are essential for ATP synthase dimer formation in yeast (30, 34). A consistent increase in oligomerization that is more evident in cybrids was found in L156R mitochondria. This suggests the interesting possibility that enzyme oligomerization may be upregulated as a compensatory response to the mutation, because the oligomeric enzyme could be more stable and/or more efficient to carry out ATP synthesis.

Taken together, our data show that it is possible to obtain a fully assembled but catalytically inhibited F_1F_0-ATP synthase from homoplasmic NARP/MILS mitochondria. Therefore, the L156R/L156P mutations *per se* do not impair the assembly route of the human F_1F_0-ATP synthase. Our results are in apparent contrast with the large amounts of sub-assembled F_1F_0 complexes found previously with BN-PAGE of T8993G mutant samples (25–27). However, most of those studies did not address whether *ATP6* mutations directly impair enzyme assembly, because they used postmortem (26) or biopsy muscular tissues (25), which have sustained metabolic stress because of disease and tissue extraction. On the other hand, when assembly was addressed in different T8993G cybrid lines (27), sub-assembled complexes were found only in some lines, although they all harbored the mutation. We consider that our results can be reconciled with the previous reports by assuming that either tissue-specific factors or mitochondrial damage during disease or sample extraction/preparation results in F_1F_0 disassembly. Thus enzyme disassembly would not be solely caused by the T8993G mutation, rather, it would be the result of a number of possible destabilizing factors.

In this line, we also showed that nonphysiological conditions such as sonication or mild heating destabilized the mutant enzyme more than the wild type. Although this instability conferred by the L156R mutation is in agreement with previous findings in *ex vivo* tissues (25, 26), it does not lead to enzyme disassembly in homoplasmic T8993G human mitochondria carrying out ATP synthesis at 40% of the wild type rate. F_1F_0 disassembly, as observed in the mutant mitochondria, was forced by our *in vitro* conditions (sonication, heating in the presence of detergents, or high salt and pH).

Our data show that the primary pathogenic mechanism of the studied NARP/MILS mutations is a decreased ATP synthesis turnover in a fully assembled and tightly coupled F_1F_0 complex. Given that the wild type and mutant mitochondria had comparable amounts of assembled F_1F_0, the inhibition in enzyme turnover is likely the result of a homogeneous population of assembled mutant enzymes working at half their capacities as a consequence of proton flow blockade through F_0, as has been proposed (6, 7, 9). A similar (59%) inhibition was observed in maximal ATPase turnover conditions (Fig. 6*A*, *closed versus open circles*). The enzyme disassembly observed in these conditions (Fig. 7) does not account entirely for the decrease in F_1F_0 ATPase rates, because the activities measured in Fig. 6 retained oligomycin sensitivity. Thus, as suggested before (6, 7, 9), these *ATP6* mutations could slow rotation of the whole central rotor because of their location at the rotor/stator interface of F_0 between subunit 6 and the ring of c subunits where protons are translocated.

More studies are required to determine the role of enzyme instability in NARP/MILS progression. Enzyme disassembly

may occur *in vivo* in metabolically demanding conditions. *ATP6* mutations hyperpolarize mitochondria (9, 20), and this ultimately leads to an increase in the production of reactive oxygen species (20). If these effects are extended into a chronic mitochondrial damage during long lasting illness, disassembly of mutant F_1F_0 may occur, as a side effect of the mutation.

Finally, by determining the mechanism of *ATP6* mutations in homoplasmic cells derived from NARP/MILS patients, this work provides key elements to develop novel gene therapy strategies to overcome the functional and destabilizing consequences of these mutations on the human ATP synthase.

Acknowledgments—We thank Professors Brian Robinson and Rosalba Carrozzo for generous cell culture donations and Professors Diego González-Halphen and Marietta Tuena de Gómez-Puyou for helpful discussions. The suggestions of Dr. Lenin Domínguez are also acknowledged.

REFERENCES

1. Tatuch, Y., Christodoulou, J., Feigenbaum, A., Clarke, J. T., Wherret, J., Smith, C., Rudd, N., Petrova-Benedict, R., and Robinson, B. H. (1992) *Am. J. Hum. Genet.* **50,** 852–858
2. Santorelli, F. M., Shanske, S., Macaya, A., DeVivo, D. C., and DiMauro, S. (1993) *Ann. Neurol.* **34,** 827–834
3. Holt, I. J., Harding, A. E., Petty, R. K., and Morgan-Hughes, J. A. (1990) *Am. J. Hum. Genet.* **46,** 428–433
4. Majander, A., Lamminen, T., Juvonen, V., Aula, P., Nikoskelainen, E., Savontaus, M. L., and Wikstrom, M. (1997) *FEBS Lett.* **412,** 351–354
5. Fryer, A., Appleton, R., Sweeney, M. G., Rosenbloom, L., and Harding, A. E. (1994) *Arch. Dis. Child.* **71,** 419–422
6. Vazquez-Memije, M. E., and García, J. J. (2002) in *Recent Research Developments in Human Mitochondrial Myopathies* (Garcia, J. J., ed) pp. 127–150, Research Signpost, Trivandrum, India
7. Schon, E. A., Santra, S., Pallotti, F., and Girvin, M. E. (2001) *Semin. Cell Dev. Biol.* **12,** 441–448
8. Vazquez-Memije, M. E., Shanske, S., Santorelli, F. M., Kranz-Eble, P., DeVivo, D. C., and DiMauro, S. (1998) *J. Inherit. Metab. Dis.* **21,** 829–836
9. Garcia, J. J., Ogilvie, I., Robinson, B. H., and Capaldi, R. A. (2000) *J. Biol. Chem.* **275,** 11075–11081
10. Carrozzo, R., Tessa, A., Vazquez-Memije, M. E., Piemonte, F., Patrono, C., Malandrini, A., Dionisi-Vici, C., Vilarinho, L., Villanova, M., Schagger, H., Federico, A., Bertini, E., and Santorelli, F. M. (2001) *Neurology* **56,** 687–690
11. Baracca, A., Barogi, S., Carelli, V., Lenaz, G., and Solaini, G. (2000) *J. Biol. Chem.* **275,** 4177–4182
12. Tatuch, Y., and Robinson, B. H. (1993) *Biochem. Biophys. Res. Commun.* **192,** 124–128
13. Hartzog, P. E., and Cain, B. D. (1993) *J. Biol. Chem.* **268,** 12250–12252
14. Carrozzo, R., Murray, J., Capuano, O., Tessa, A., Chichierchia, G., Neglia, M. R., Capaldi, R. A., and Santorelli, F. M. (2000) *Neurol. Sci.* **21,** Suppl. 5, S983–S984
15. Ogilvie, I., and Capaldi, R. A. (1999) *FEBS Lett.* **453,** 179–182
16. Santorelli, F. M., Shanske, S., Jain, K. D., Tick, D., Schon, E. A., and DiMauro, S. (1994) *Neurology* **44,** 972–974
17. Santorelli, F. M., Mak, S. C., Vazquez-Memije, E., Shanske, S., Kranz-Eble, P., Jain, K. D., Bluestone, D. L., De Vivo, D. C., and DiMauro, S. (1996) *Pediatr. Res.* **39,** 914–917
18. Fujii, T., Hattori, H., Higuchi, Y., Tsuji, M., and Mitsuyoshi, I. (1998) *Pediatr. Neurol.* **18,** 275–277
19. de Vries, D. D., van Engelen, B. G., Gabreels, F. J., Ruitenbeek, W., and van Oost, B. A. (1993) *Ann. Neurol.* **34,** 410–412
20. Carrozzo, R., Rizza, T., Stringaro, A., Pierini, R., Mormone, E., Santorelli, F. M., Malorni, W., and Matarrese, P. (2004) *J. Neurochem.* **90,** 490–501
21. Garcia, J. J., Minauro-Sanmiguel, F., and Bravo, C. (2002) in *Recent Research Developments in Human Mitochondrial Myopathies* (Garcia, J. J., ed) pp. 127–150, Research Signpost, Trivandrum, India
22. Fillingame, R. H., Angevine, C. M., and Dmitriev, O. Y. (2003) *FEBS Lett.* **555,** 29–34
23. Vik, S. B., Long, J. C., Wada, T., and Zhang, D. (2000) *Biochim. Biophys. Acta* **1458,** 457–466
24. Lightowlers, R. N., Howitt, S. M., Hatch, L., Gibson, F., and Cox, G. B. (1987) *Biochim. Biophys. Acta* **894,** 399–406
25. Carrozzo, R., Wittig, I., Santorelli, F. M., Bertini, E., Hofmann, S., Brandt, U., and Schagger, H. (2006) *Ann. Neurol.* **59,** 265–275
26. Houstek, J., Klement, P., Hermanska, J., Houstkova, H., Hansikova, H., Van den Bogert, C., and Zeman, J. (1995) *Biochim. Biophys. Acta* **1271,** 349–357
27. Nijtmans, L. G., Henderson, N. S., Attardi, G., and Holt, I. J. (2001) *J. Biol. Chem.* **276,** 6755–6762
28. Aggeler, R., Coons, J., Taylor, S. W., Ghosh, S. S., Garcia, J. J., Capaldi, R. A., and Marusich, M. F. (2002) *J. Biol. Chem.* **277,** 33906–33912
29. Schagger, H., and von Jagow, G. (1991) *Anal. Biochem.* **199,** 223–231
30. Arnold, I., Pfeiffer, K., Neupert, W., Stuart, R. A., and Schagger, H. (1998) *EMBO J.* **17,** 7170–7178
31. Schagger, H., and Pfeiffer, K. (2000) *EMBO J.* **19,** 1777–1783
32. Minauro-Sanmiguel, F., Wilkens, S., and Garcia, J. J. (2005) *Proc. Natl. Acad. Sci. U. S. A.* **102,** 12356–12358
33. Krause, F., Reifschneider, N. H., Goto, S., and Dencher, N. A. (2005) *Biochem. Biophys. Res. Commun.* **329,** 583–590
34. Paumard, P., Vaillier, J., Coulary, B., Schaeffer, J., Soubannier, V., Mueller, D. M., Brethes, D., di Rago, J. P., and Velours, J. (2002) *EMBO J.* **21,** 221–230
35. Bravo, C., Minauro-Sanmiguel, F., Morales-Rios, E., Rodriguez-Zavala, J. S., and Garcia, J. J. (2004) *J. Bioenerg. Biomembr.* **36,** 257–264
36. Trautschold, I. L. W., and Schweitzer, G. (1995) in *Methods of Enzymatic Analysis* (Bergmeyer, H. U., ed) Verlagsgesellschaft, Weinheim, Germany
37. Peterson, G. L. (1977) *Anal. Biochem.* **83,** 346–356
38. Laemmli, U. K. (1970) *Nature* **227,** 680–685
39. Ko, Y. H., Delannoy, M., Hullihen, J., Chiu, W., and Pedersen, P. L. (2003) *J. Biol. Chem.* **278,** 12305–12309
40. Sgarbi, G., Baracca, A., Lenaz, G., Valentino, L. M., Carelli, V., and Solaini, G. (2006) *Biochem. J.* **395,** 493–500
41. García, J. J., Morales-Ríos, E., Cortés-Hernández, P., and Rodríguez-Zavala, J. S. (2006) *Biochemistry* **45,** 12695–12703